A Fully Coupled Model of Non-linear Wave in a Harbor

Daguo Wang[1]

Abstract: A 2-D time-domain numerical coupled model for non-linear wave forces acting on a fixed ship is developed in the present study. The whole domain is divided into the inner domain and the outer domain. The inner domain is the area around the ship section and the flow is described by the Laplace equation. The remaining area is the outer domain and the flow is defined by the higher-order Boussinesq equations in order to consider the nonlinearity of the wave motions. The matching conditions on the interfaces between the inner domain and the outer domain are the continuation of volume flux and the equality of wave elevations. The procedure of coupled solution, the length of common domain and the calculation region of the inner domain are discussed in detail. The physical experiment, including the wave flume and the waves acting on a fixed ship, the boundary element method in complex and the Boussinesq equations are conducted to validate the present model, and it is shown that the numerical results of the present model agree well with the experimental data and the other numerical results, but the computational efficiency of the present model is much higher than that of the boundary element method in complex, so the present model is efficient and accurate, which can be used for the study on the effect of the nonlinear wave forces acting on a fixed ship or other structures in a large harbor.

Keywords: Boussinesq equations, Laplace equation, coupled model, non-linear wave forces

1 Introduction

There are two common approaches, namely potential theory and Navier-Stokes (N-S) theory, to calculate nonlinear wave forces acting on a body. In the potential theory, the Laplace equation for velocity potential under nonlinear boundary conditions can be solved by the boundary element method (BEM) [Lin, Newman and

---

[1] School of Environment and Resource, Southwest University of Science and Technology, Mianyang 621010, China.
Corresponding author. Email address: dan_wangguo@163.com

Yue (1984); Boo, Kim and Kim (1994); Celebl, Kim and Beck (1998)] or finite element method [Wu and Eatock (1994); Turnbull, Borthwick and Eatock (2003); Wang, Zou and Liu (2010)]. The N-S Equations are solved numerically with the marker and cell method (MAC) [Park and Kim (1998)], the volume of fluid method (VOF) [Hirt and Nichols (1981)] or the smoothed particle hydrodynamics (SPH) [Moulinec, Issa, Marongiu and Violeau (2008)]. The above two approaches can only be applied to small computational region because tremendous computation time is needed. For harbor engineering, one has to compute the nonlinear wave forces acting on ships moored in a harbor. For such a case, the wave motions for the whole harbor have to be considered since the waves in the harbor will undergo reflections from the harbor boundaries and refractions on the varying bottom of the harbor. Since the nonlinearity of water waves is enhanced by the shallow water, the nonlinear wave forces also become more complex compared to the open sea condition. The commonly used methods of ship motions in a harbor [Van Oortmerssen (1976); Zou and Bowers (1993)] can not consider these requirements. Adopting the depth-averaged simplification, Boussinesq equations [Peregrine (1967); Nwogu (1993); Wei, Kirby, Grilli and Subramanya (1995); Madsen, Bingham and Liu (2002); Hsu, Hsiao, Ou, Wang, Yang and Chou (2007)], which turn 3-D problems into 2-D ones, are commonly used for the harbor waves because of their nonlinear feature and efficiency for large computational domains. However, the 3-D characteristics of fluid motions in the vicinity of the ship hull can not be taken into account by this model. Therefore, coupled models have been developed to overcome these shortcomings. Takagi, Naito and Hirota (1994) simulated the interaction between ship and waves by a coupled model, in which the outer domain was governed by the mild-slope equations and the inner domain was numerically solved by the 3-D boundary element method. Jiang (1998) simulated ship waves in shallow water by a coupled model. Boussinesq type equations were used both in the inner domain beneath the ship and the outer domain. Bingham (2000) applied the Boussinesq equations to calculate the waves in the harbor without considering the ship and used this result as the incident waves for the moored-ship motion which was modeled by the linear potential theory (source distribution method). Therefore, the nonlinear interaction between ship and waves could not be fully taken into account in the method. Qi, Wang and Zou (2000); Qi, Zou and Wang (2000) developed a coupled model for numerical simulations of nonlinear waves. In the approach, the outer domain was defined by the Boussinesq equations and the inner domain was defined by the N-S equations. Wang and Zou (2007) simulated the nonlinear wave forces acting on a fixed ship section against a vertical quay by developing a coupled model, in which the outer domain was expressed by the Boussinesq equations and the inner domain was described by the Newton's second law. Hamidou, Molin, Kadri, Kimmoun and Tahakourt (2009) proposed a 2-D coupling method

between extended Boussinesq equations and the integral equation method. In the method, there was no common domain between the inner domain and the outer domain, and its matching conditions were relatively complex. Wang, Zou, Tham and Liu (2010); Wang, Zou and Tham (2011) simulated wave forces on a fixed-boxed ship by a coupled model, in which the flow in the outer domain was governed by the Boussinesq equations and the flow in the inner domain was governed by the simplified linear Euler equations, but the model can not consider the 3-D characteristics of fluid motions in the vicinity of the ship hull.

In the present paper, a 2-D nonlinear wave coupled model is developed. The physical experiment and the other numerical models are adopted to validate the present model. In Section 2, the governing equations are illustrated. The matching conditions and the solution procedure are discussed in Section 3-4 respectively. In Section 5 and Section 6, the physical experiment is described and the calculation region of the inner domain is discussed respectively. The computational results are carried out in Section 7 and the computational efficiency of the present model is reported in Section 8.
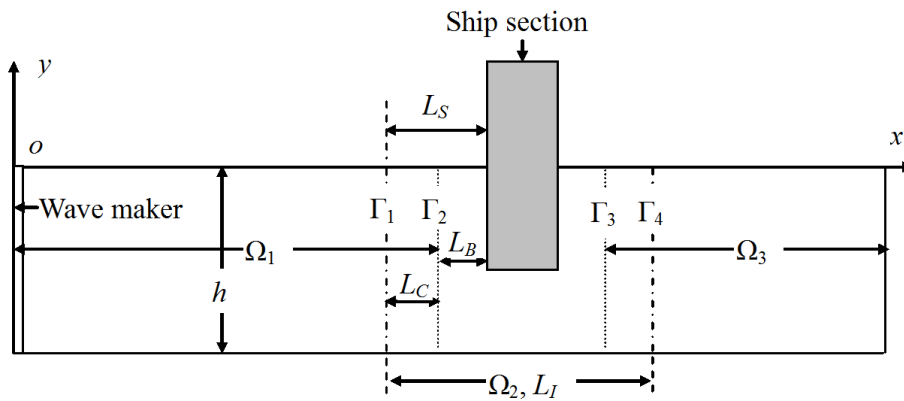
2 Governing equations

Figure 1: Schematic diagram of the coupled model (where h is the still water depth, Γ_1 is the left boundary of the inner domain Ω_2, Γ_2 is the right boundary of the outer domain Ω_1, Γ_3 is the left boundary of the outer domain Ω_3, Γ_4 is the right boundary of the inner domain Ω_2, L_C is the common length between the inner domain and the outer domain, L_B is the distance between the interfaces (Γ_2 and Γ_3) and the ship, L_S is the distance between the interfaces (Γ_1 and Γ_4) and the ship, and L_I is the calculation region in the $x-$direction of the inner domain)

As shown in Fig.1, the origin of a Cartesian coordinate system is on the mean surface with the *x*-axis pointing to the propagation direction of incoming waves and the *y*-axis pointing to the opposite direction of gravity. The entire fluid domain is divided into three domains: the inner domain Ω_2 and the outer domain Ω_1 & Ω_3 . The inner domain is the area around the ship section, where flow is expressed by the Laplace equation. The remaining area is the outer domain, where flow is expressed by the higher-order Boussinesq equations.

2.1   Governing equations of the outer domain

The governing equations in the outer domain Ω_1 and Ω_3 are given by the 1-D form of the higher-order Boussinesq equations [Zou (1999)], that is

$$\zeta_t + [(h+\zeta)\bar{u}]_x = 0, \tag{1}$$

$$\bar{u}_t + \bar{u}\bar{u}_x + g\zeta_x + G = \frac{1}{3}h^2\bar{u}_{xxt} + B_1h^2\left(\bar{u}_t + g\zeta_x\right)_{xx} + B_2\left(h^2\bar{u}_t + gh^2\zeta_x\right)_{xx}, \tag{2}$$

$$G = \left\{ \begin{array}{l} \frac{(h+\zeta)^2}{3}\left[(\bar{u}_x)^2 - \bar{u}\bar{u}_{xx} - \frac{1}{10}(\bar{u}\bar{u})\right] \\ +\frac{1}{3}(h+\zeta)\zeta_x\left[(\bar{u}_x)^2 - \bar{u}\bar{u}_{xx}\right] - (h+\zeta)\zeta_x\bar{u}_{xt} - \frac{1}{3}\zeta(2h+\zeta)\bar{u}_{xxt} \end{array} \right\}_x, \tag{3}$$

where ζ is the wave elevation, g is the gravity acceleration, t is the time, $\bar{u}$ is the depth-averaged horizontal velocity. B_1 and B_2 are two parameters and $B_1 + B_2 = 1/15$. Taking $B_2 = 2/59$ will give the optimal shoaling property of the equations. The accuracy of Eqs. (1) and (2) is third order, and the dispersion is accurate to the $0\left(\mu^4\right)$ and nonlinearity to the $0\left(\varepsilon\mu^2\right)$ ($\mu = h/L_0$, $\varepsilon = A/h$, L_0 is a characteristic wave length and A is a characteristic wave amplitude).

Eqs. (1) and (2) can be discretized on a rectangle space-staggered grid system with the depth-averaged velocity $\bar{u}$ defined at the time level n and the wave elevation ζ at time level $n - \frac{1}{2}$, and solved numerically by the Predictor-Corrector scheme using the finite difference method [Zou and Xu (1998)].

2.2   Governing equation of the inner domain

The governing equation of the inner domain is

$$\beta(z,t) = \phi(z,t) + i\psi(z,t), \tag{4}$$

where ϕ is the velocity potential and ψ is the stream function, which satisfy Laplace equation respectively, and $z = x + iy$ is applicable for describing the fluid motion.

On the instantaneous free surface, both the fully nonlinear kinematic and dynamic boundary conditions must be satisfied

$$\frac{\partial \phi}{\partial \zeta} = \frac{\partial \zeta}{\partial t} + \frac{\partial \phi}{\partial t}\frac{\partial \zeta}{\partial x}, \tag{5}$$

$$g\zeta + \frac{\partial \phi}{\partial t} + \frac{1}{2}\nabla\phi\cdot\nabla\phi = 0. \tag{6}$$

Eq. (4) and (5) can be written in the following semi-Lagrangian form

$$\frac{\delta\zeta}{\delta t} = \frac{\partial\phi}{\partial y} - \frac{\partial\phi}{\partial x}\frac{\partial\zeta}{\partial x}, \tag{7}$$

$$\frac{\delta\phi}{\delta t} = -g\zeta - \frac{1}{2}\nabla\phi\cdot\nabla\phi + \frac{\delta\zeta}{\delta t}\frac{\partial\phi}{\partial y}, \tag{8}$$

where $\frac{\delta}{\delta t} = \frac{\partial}{\partial t} + \vec{V_p}\cdot\nabla$, $\vec{V_p} = \left(0, \frac{\delta\zeta}{\delta t}\right)$. Eq. (4) was solved by boundary element method to successfully simulate the 2-D non-linear wave flume in [Lin, Newman, and Yue (1984)]. Using the boundary element method (BEM), non-linear wave forces acting on ship section were calculated in [Wang, Chen and Tang (2009)]. In the present paper, with the method, the inner domain of the coupled model is simulated.

3   Matching conditions

As shown in Fig. 1, there are four interfaces between the inner domain and the outer domain. The matching conditions on the interfaces Γ_1 and Γ_4 are the continuation of volume flux

$$\psi_j(i) = \int_{-h}^{y_j(i)} u_j(i)\,dy \qquad j = 1,4, \tag{9}$$

where $\psi_j(i)$ is the stream function of each node on the matching interfaces Γ_1 and Γ_4, which can be given by the solution of the inner domain Ω_2. $y_j(i)$ is the vertical coordinate of each node at the interfaces Γ_1 and Γ_4 along water depth, which can be determined by the following equation

$$y(i) = \zeta^* - \frac{(h+\zeta^*)}{(N-1)}(i-1) \quad (i = 1,2,\cdots N), \tag{10}$$

where ζ^* is the wave elevations at the interfaces Γ_1 and Γ_4, which can be given by the solution of the outer domain Ω_1 and Ω_3, and N is the number of nodes of the inner domain at the interfaces Γ_1 and Γ_4. The $u_j(i)$ in Eq. (9) is the horizontal

velocities at the interfaces Γ_1 and Γ_4 and it is obtained by the solution of the outer domain Ω_1 and Ω_3. From Eqs. (1) and (2), the $u_j(i)$ is a fourth order polynomial [Zou (1999)]

$$
\begin{aligned}
u(i) = \bar{u} - \tfrac{1}{2} \left[(h+y(i))^2 - \tfrac{(h+\zeta^*)^2}{3} \right] \bar{u}_{xx} \\
+ \tfrac{1}{24} \left[(h+y(i))^4 - 2(h+y(i))^2 (h+\zeta^*)^2 + \tfrac{7}{15} (h+\zeta^*)^4 \right] \bar{u}_{xxxx}
\end{aligned}
\tag{11}
$$

The matching conditions on the interfaces Γ_2 and Γ_3 are the continuation of volume flux

$$
\bar{u}_j = \frac{\psi_j}{(h+y_j)} \qquad j = 2,3,
\tag{12}
$$

and the equality of wave elevations

$$
\zeta_j = y_j \qquad j = 2,3,
\tag{13}
$$

where $\bar{u}_j$ and ζ_j are the depth-averaged horizontal velocities and wave elevations at the interfaces Γ_2 and Γ_3, respectively, which are given by the solution of the outer domain Ω_1 and Ω_3. ψ_j and y_j are the stream function and wave elevations at the interfaces Γ_2 and Γ_3, respectively, which are determined by the solution of the inner domain Ω_2.

It should be pointed out that the matching conditions (9), (12) and (13) obey mass conservation, which shows that the present coupled model is a fully coupled one.

4   Solution procedure

The solution procedure of the present model includes the following steps. The first step: Firstly, the $\bar{u}_2$ and ζ_2, which are the right boundary conditions of the outer domain Ω_1, can be obtained by Eq. (12) and (13). With the boundary conditions and the incident boundary condition, the Boussinesq equations can be solved in the outer domain Ω_1. Then, the $\psi_1(i)$ and $\psi_4(i)$, which are the left and right boundary conditions of the inner domain Ω_2, can be given by Eq. (9). Using the boundary conditions, Eq. (4) can be calculated in the inner domain Ω_2. Lastly, through Eq. (12) and (13), we can obtain the $\bar{u}_3$ and ζ_3, which are the left incident boundary conditions of the outer domain Ω_3. With the boundary conditions and open condition, the Boussinesq equations can be solved in the outer domain Ω_3.

The second step: By compared the velocity in the inner domain with the velocity in the outer domain at the same position in the common domain, the iteration is finished and the next time step begins if the relative error between them is less than 1%, otherwise the computation procedure is repeated.

5   Physical experiment

The physical experiment was conducted in a wave flume of 46 m in length, 0.7m in width and 1m in depth at the State Key Laboratory of Coastal and Offshore Engineering, Dalian University of Technology, China. Incident waves were generated by a wave maker from one end of the wave flume. The ship model had a width $B = 0.6$m and length $L = 0.4$m. The height was 0.45 m. It was placed 27.4m away from the wave maker (see Fig. 2) and fixed by a support bar. As shown in Fig. 3, two boxes of 0.147 m in width were placed at the two sides of the ship model with a gap of 0.003 m between the boxes and the ship model in order to avoid the friction between them.

Wave elevations were measured by wave gauges as shown in Fig. 2. Horizontal and vertical wave forces acting on the ship model were measured by a force sensor, which was placed in the centre of the ship top as shown in Figs. 2-4. Pressure sensors were also installed on the surface of the ship model (see Fig. 4) and the locations of these pressure sensors are given in Tab. 1.

Sine waves were generated by the wave maker and the motion of the wave maker paddle is defined by

$$S = S_a \sin wt \qquad (14)$$

where S_a and w is the stroke length and the frequency of wave maker paddle respectively. Six cases were studied in the experiment (Shown in Tab. 2).
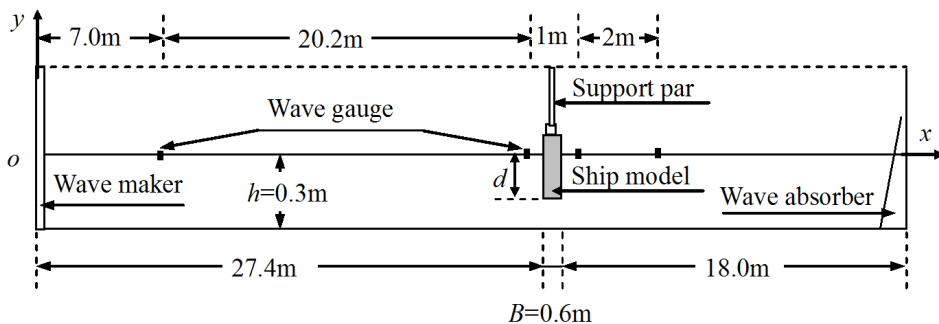
Figure 2: Experimental setup (where d is the draft of the ship model)
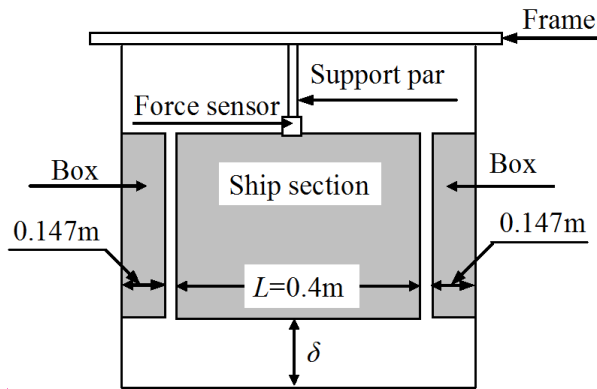
Figure 3: Wave flume cross section (where δ is the gap width between the ship bottom and the seabed)
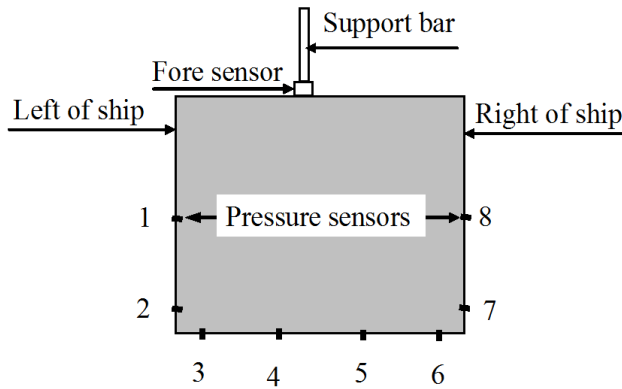
Figure 4: Pressure sensor setup

Table 1: Positions of the pressure sensors

Number of pressure sensors	1	2	7	8
Distance from bottom /m	0.18	0.02	0.02	0.18
Number of pressure sensors	3	4	5	6
Distance from left /m	0.02	0.2	0.4	0.58

Table 2: Incident wave characteristics (where H is the incident wave height and T is the incident wave period)

		Case 1	Case 2	Case 3	Case 4	Case 5	Case 6
Water depth h(m)		0.3	0.3	0.3	0.3	0.3	0.3
Wave height	H(m)	0.03	0.06	0.06	0.06	0.06	0.06
	H/h	0.1	0.2	0.2	0.2	0.2	0.2
Wave period	T(s)	2	3	5	3	3	3
	$T\sqrt{g/h}$	11.4	17.1	22.8	17.1	17.1	17.1
Draft	d (m)	0.27	0.24	0.24	0.27	0.18	0.21
	d/h	0.9	0.8	0.8	0.9	0.6	0.7

6   Calculation region of the inner domain

6.1   Length of L_C

The $\bar{u}_{xxxx}$ in Eq. (11) is fourth derivative of depth-averaged horizontal velocity to horizontal coordinate, which can be obtained from the following finite difference method

$$\bar{u}_{xxxx} = \left(\bar{u}_{i+2} - 4\bar{u}_{i+1} + 6\bar{u}_i - 4\bar{u}_{i-1} + \bar{u}_{i-2}\right)\big/(\Delta x)^4 \tag{15}$$

where Δx is the space step length of the outer domain and $\Delta x = 0.1$ in the present model, and i is the nodal label of the outer domain (see Fig. 5). From Fig. 5, the length of the common domain between the inner domain and the outer domain is

$$L_C = (N-1)(\Delta x) \tag{16}$$

where N is the nodal number of the outer domain in the common domain. Based on Eq. (15) and Fig. 5, N is not less than 4. If N is greater than 4, the computation cost will increase, so $N = 4$ and $L_C = 0.3$m.

6.2   Length of L_S

As shown in Fig. 1, the distance between the interfaces (Γ_1 and Γ_4) and the ship is

$$L_s = L_c + L_B \tag{17}$$

If L_B is too shorter, the characteristics of fluid motions around the ship section can't be accurately given by Eq. (11). If L_B is too longer, the computation cost will increase. In the present model, taking L_B as one width of the ship model gives $L_B = 0.6$m, so $L_S = 0.9$m.
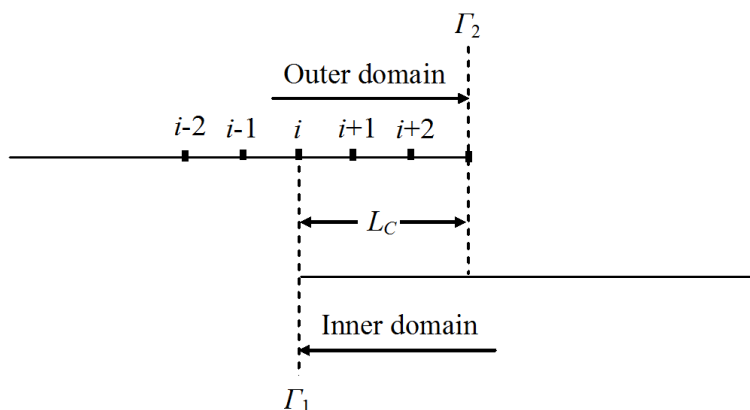
Figure 5: Length of the common domain

6.3 *Calculation region of the inner domain*

As shown in Fig. 1, the calculation region in the $x-$direction of the inner domain is

$$L_I = 2L_S + B = 2 \times 0.9 + 0.6 = 2.4m \qquad (18)$$

7 Computational results

7.1 *Computational results of wave flume*

A wave flume, which is the same as that in the physical experiment (Fig. 2), is simulated by the present coupled model and the Boussinesq equations [Zou (1999)]. As discussed in Section 6, the common length between the inner domain and the outer domain L_C is 0.3m. As shown in Fig. 6, the calculation region in the $x-$direction of the inner domain is 2.4m, the calculation region of the outer domain Ω_1 is 26.8m and the calculation region of the outer domain Ω_2 is 17.4m. The space step length [Zou (1999)] in the outer domain is 0.1m, and the space step length of the inner domain in the coupled model is 0.05m. The incident wave period is 3.0s and the incident wave height is 0.06m.

Fig. 7 shows the wave profiles at the $t = 10$, $t = 20$ and $t = 30$s, and Fig. 8 shows the time history of wave elevations at the $x = 7.0$, $x = 13.0$, $x = 19.0$, $x = 25.2$, $x = 27.2$, $x = 28.2$ and $x = 30.2$m. In Fig. 8, the computational results of the coupled model at the $x = 7.0$, $x = 13.0$, $x = 19.0$, $x = 25.2$ and $x = 30.2$m are obtained from the Boussinesq equations in the outer domain, and the computational results of the coupled model at the $x = 27.2$, $x = 28.2$m are obtained from the boundary
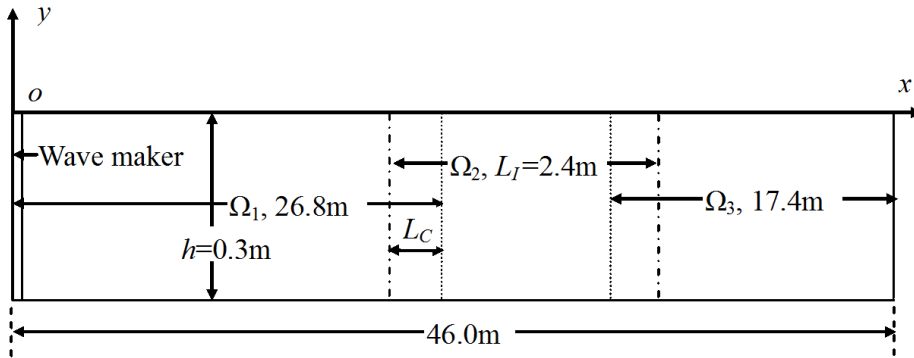
Figure 6: Wave flume

element method [Lin, Newman, and Yue (1984); Wang, Chen and Tang (2009)] in the inner domain. It can be seen from the Figs. 7-8 that the computational results of the coupled model, same as that of the Boussinesq equations, agree well with the experimental data. There are some errors between the numerical results and the experiment data in Fig. 8(g) after $t = 38$s and in Fig. 8(f) after $t = 35$s, which are caused by the wave reflection in the experiment. Therefore, the coupled model can be used to simulate accurately the propagation of nonlinear waves and it is very successful.

7.2 Computational results of waves acting on a fixed ship

The computational region and input parameters for the numerical model are the same as those in the physical experiment, which is shown in Fig. 2 and Tab. 2. The computational results and experimental data are shown in Figs. 9-11.

Figs. 9(a)-9(c) show the time series of numerical and experimental wave elevations for different wave periods. The wave period is $T =2$s in Fig. 9(a), $T =3$s in Fig. 9(b) and $T =5$s in Fig. 9(c). Fig. 9(b) and Figs. 9(d)-9(e) show the time series of numerical and experimental wave elevations for different draft of the ship model. The draft is $d =0.24$m in Fig. 9(b), $d =0.27$m in Fig. 9(d) and $d =0.18$m in Fig. 9(e).

Fig.10 shows the time series of numerical and experimental wave pressures on ship section for Case 6. In the figure, Arabic numbers denotes the number of the pressure sensors, pressure sensors 1-2 are placed on the left side of the ship model, 3-6 on the bottom of the ship model, and 7-8 on the right side of the ship model, and ρ is the water density.

Figs. 11 show the time series of numerical and experimental wave forces on the

ship section for Case 1 to Case 5.

From the Figs. 9-11, it can be seen that the numerical results of the coupled model,
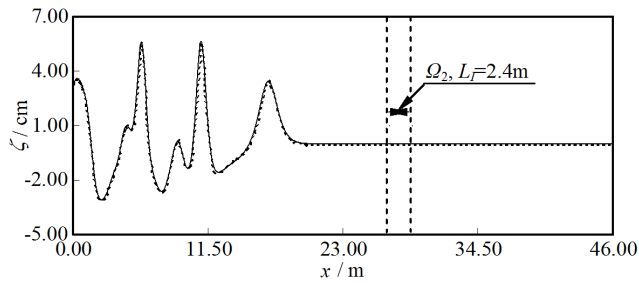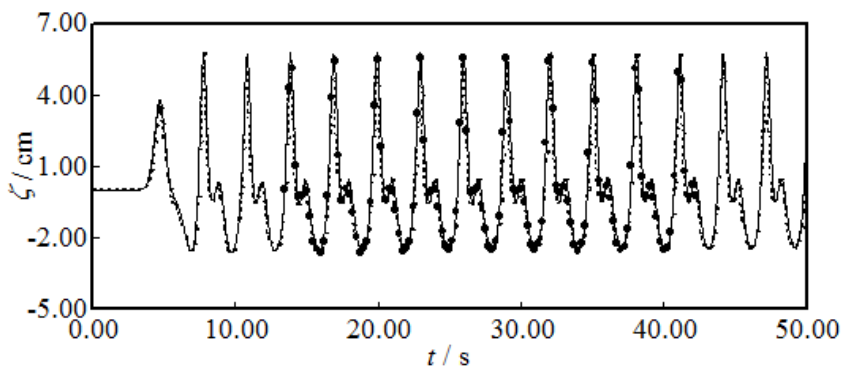

(a) Wave profile at $t = 10$s
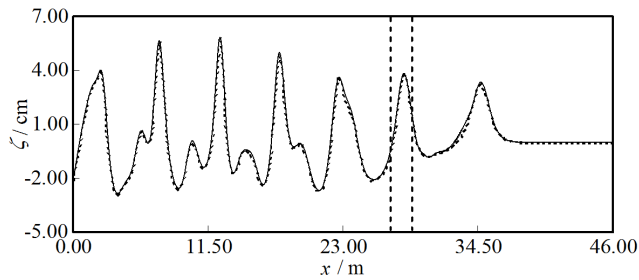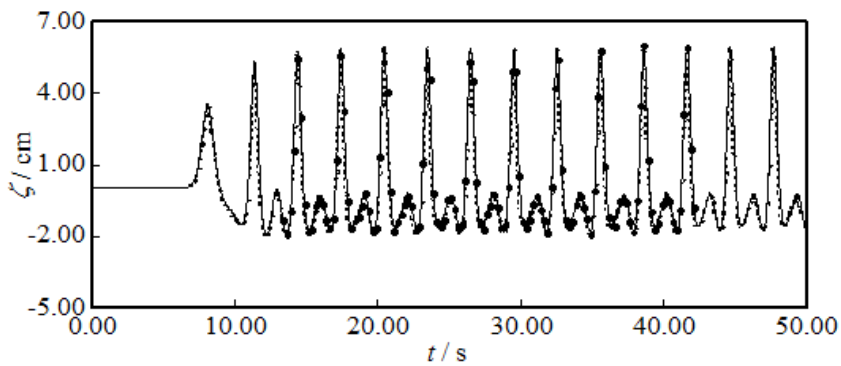

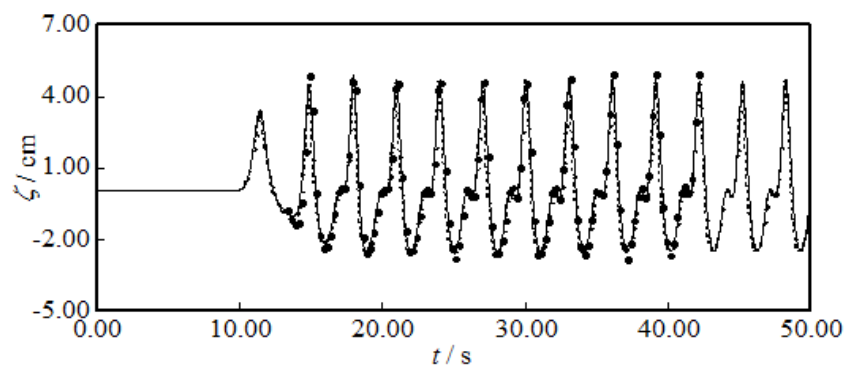(b) Wave profile at $t = 20$s
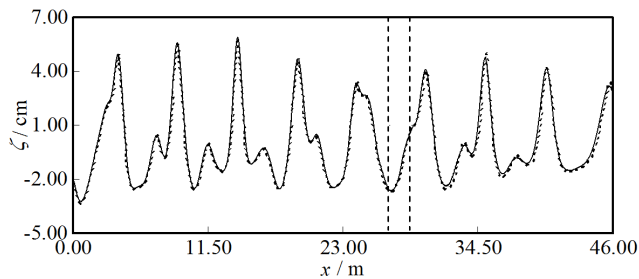
(c) Wave profile at $t = 30$s

Figure 7: Wave profiles at different instant (where dashed lines are the Boussinesq equations [Zou (1999)] results and solid lines are the coupled mode results)
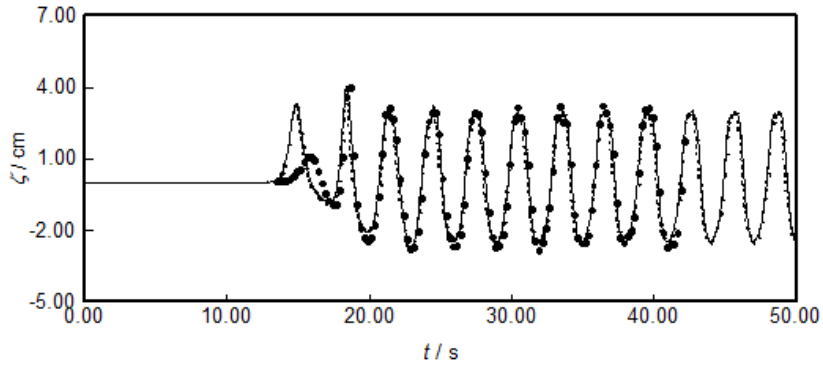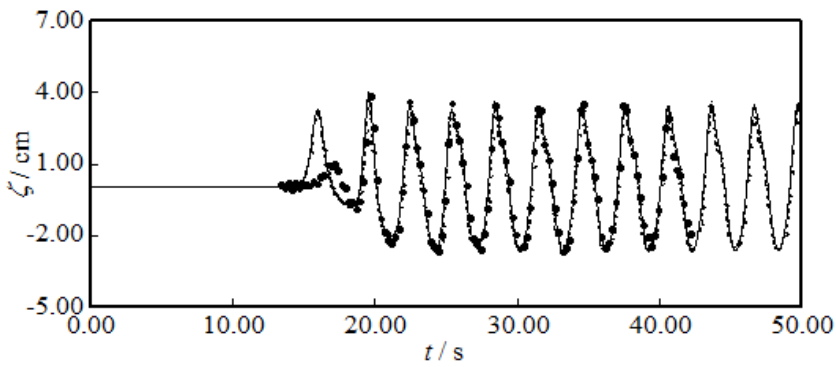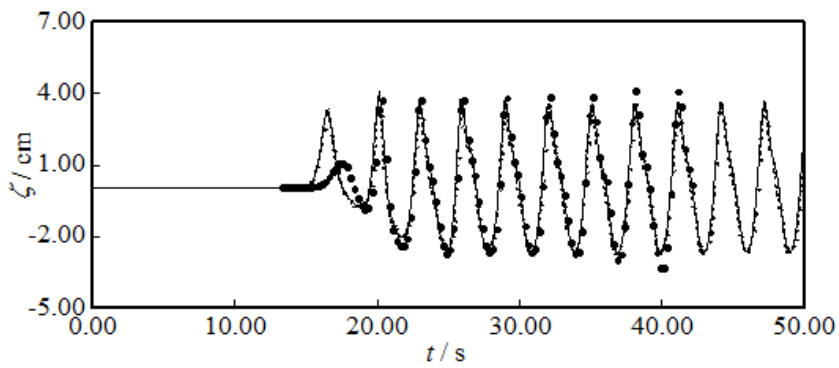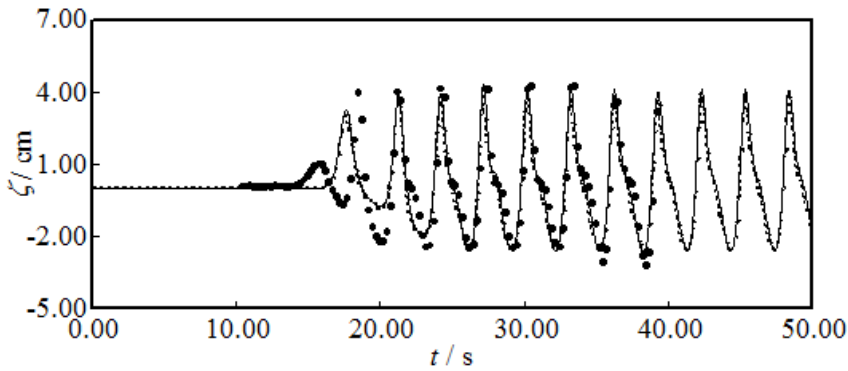
(a) Time history of wave elevations at $x=7.0\text{m}$

(b) Time history of wave elevations at $x=13.0\text{m}$

(c) Time history of wave elevations at $x=19.0\text{m}$

(d) Time history of wave elevations at *x*=25.2m

(e) Time history of wave elevations at *x*=27.2m


(f) Time history of wave elevations at *x*=28.2m

(g) Time history of wave elevations at *x*=30.2m

Figure 8 : Time history of wave elevations at the different position (where *x* is the position of the wave gauges away from the incident boundary, markers are experimental data, dashed lines are the Boussinesq equations [Zou (1999)] results and solid lines are the coupled mode results)
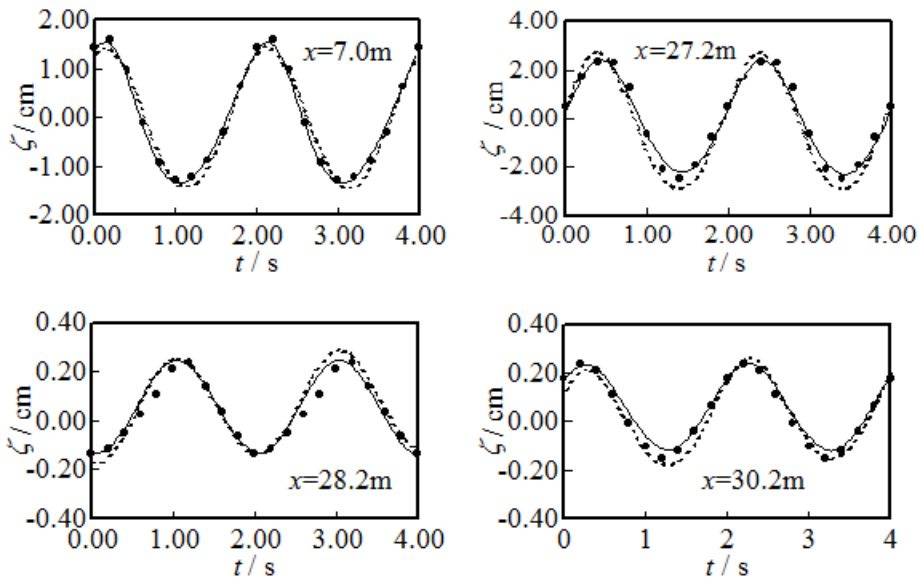
(a) Case1: *T*=2s, *H*=0.03m, *d*=0.27m
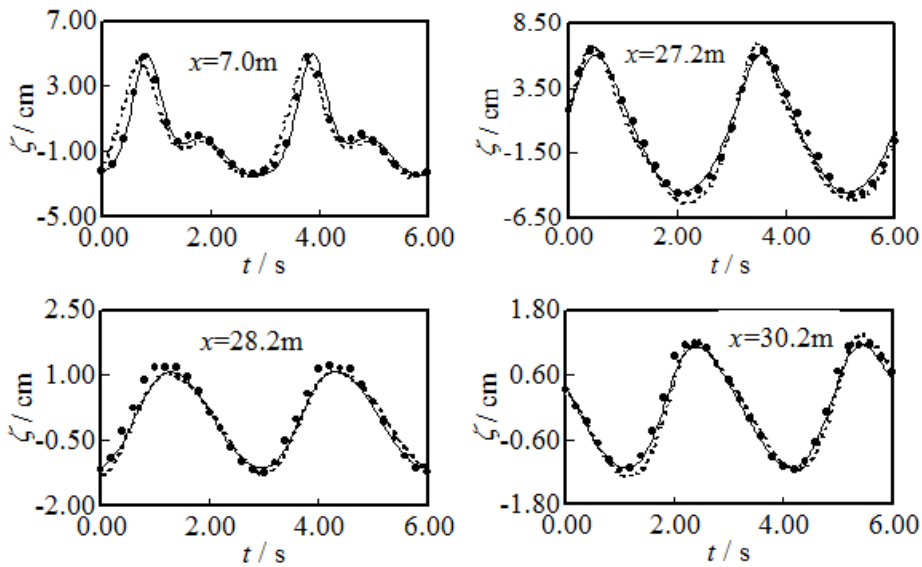
(b) Case2: T=3s, H=0.06m, d=0.24m
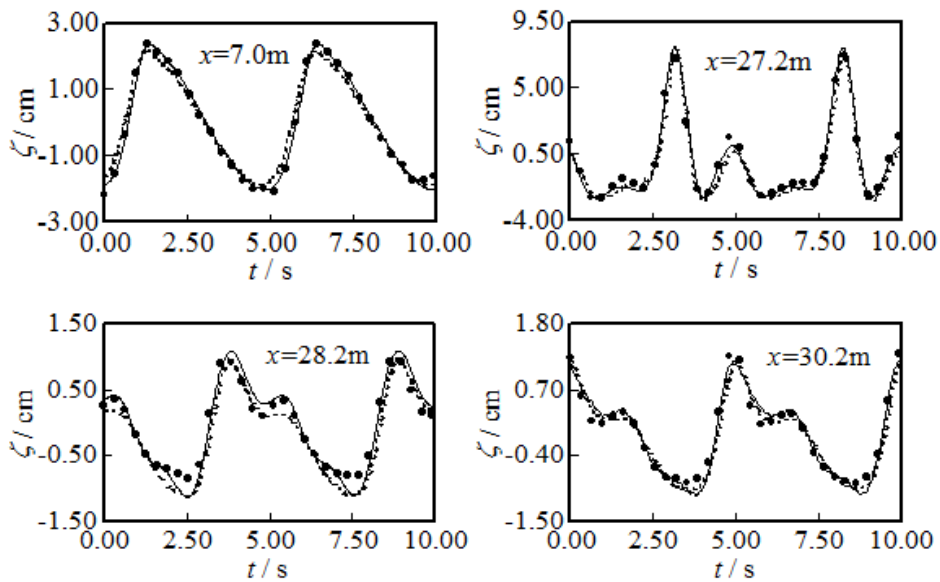
(c) Case3: T=5s, H=0.06m, d=0.24m
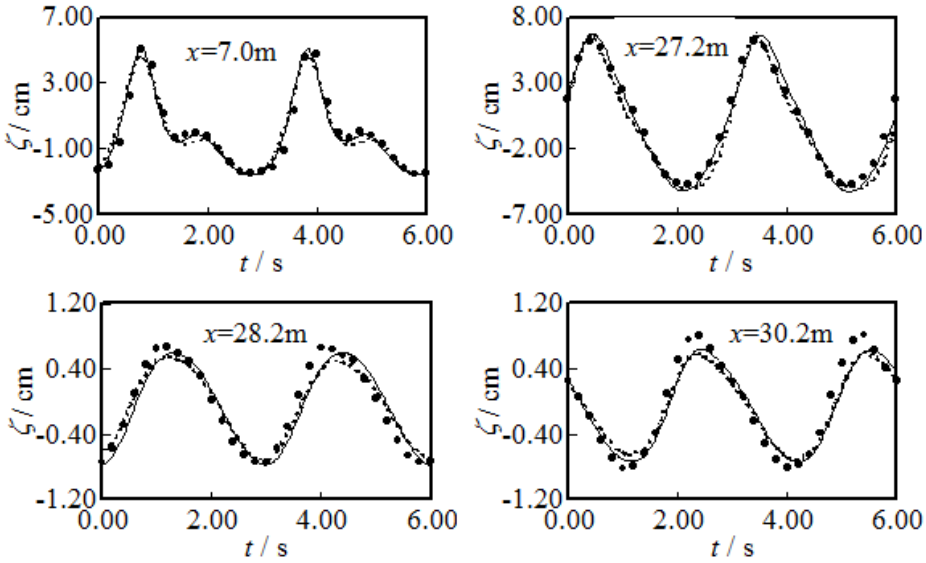
(d) Case4: T=3s, H=0.06m, d=0.27m

which are the same as that of the boundary element method in complex [Lin, Newman, and Yue (1984); Wang, Chen and Tang (2009)], agree well with the experimental data.

8   Computational efficiency of two numerical models

For a comparison of the computational efficiencies between the present model and the boundary element method in complex [Lin, Newman, and Yue (1984); Wang, Chen and Tang (2009)], the fluid domain in Fig. 2 was calculated on a PIV-2.4GHZ computer with 1G RAM by the two models. The incident wave period and wave height were $T = 2$s, $H = 0.03$m, respectively. The computational times of the two models are listed in Tab. 3.

Table 3: Computational time of the two models

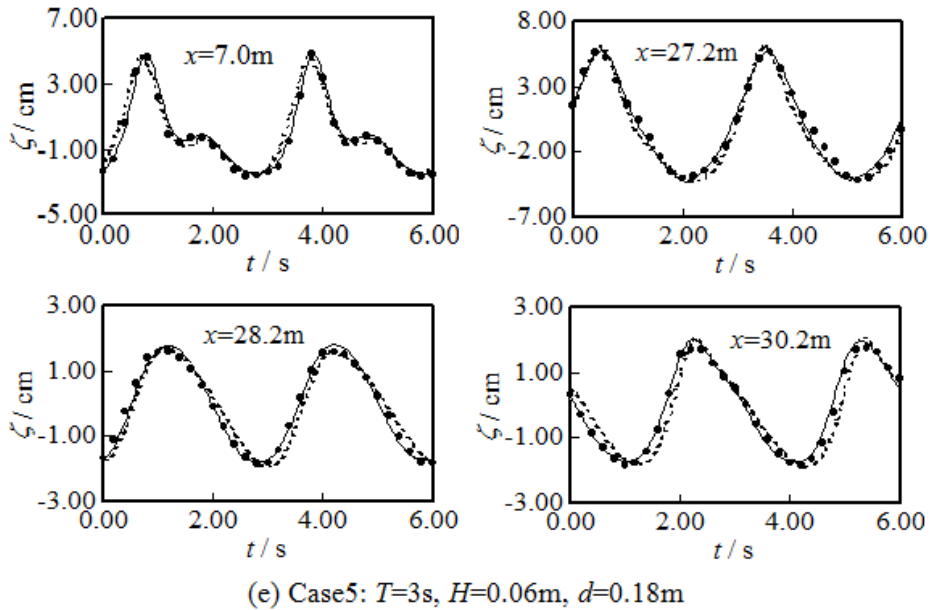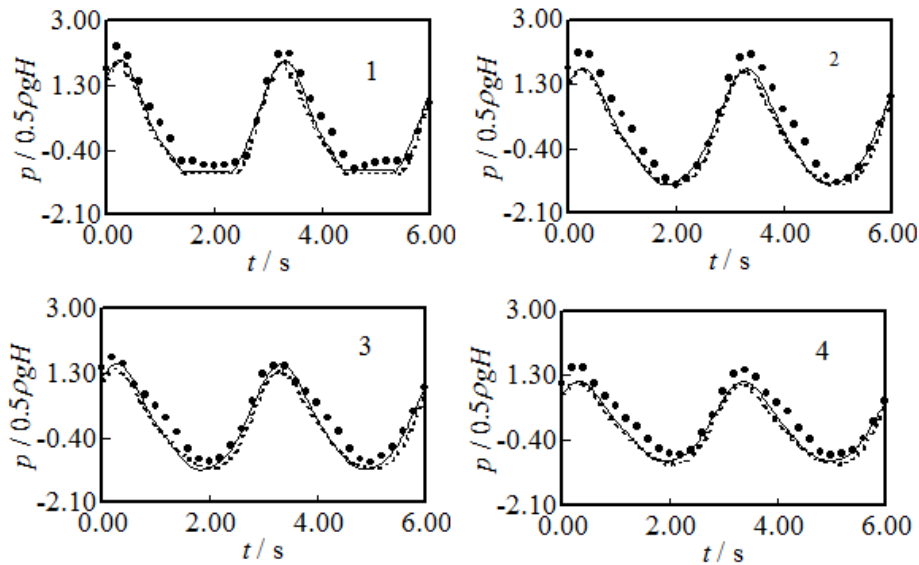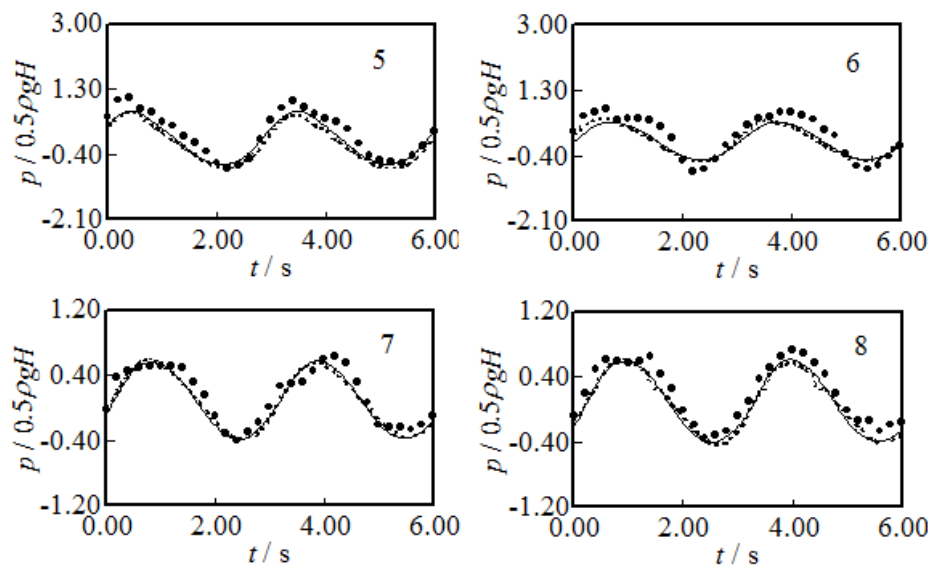|	BEM	Coupled model
Space step length	$\Delta x = 0.05$m	$\Delta x = 0.05$m in inner domain; $\Delta x = 0.1$m in outer domain
Total computational steps	1800	1800
Total computational time	567.09ks	9.40ks

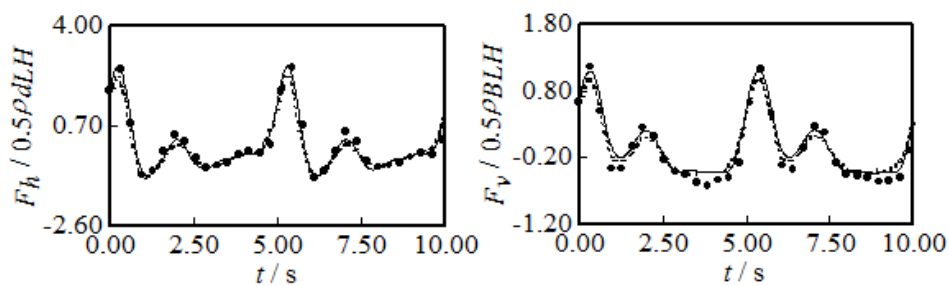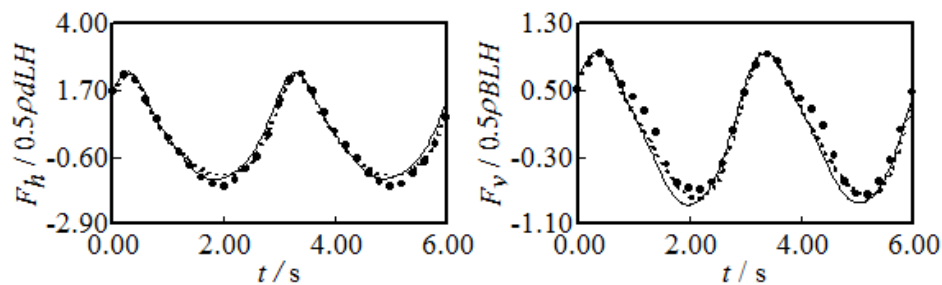(e) Case5: T=3s, H=0.06m, d=0.18m

Figure 9 : Time history of wave elevations (where x is the horizontal coordinate of wave gauges, markers are the experimental data, dashed lines are the BEM [Lin, Newman, and Yue (1984); Wang, Chen and Tang (2009)] results and solid lines are the coupled mode results)

Case6: *T*=3s, *H*=0.06m, *d*=0.21m

Figure 10 : Time history of wave pressures (where markers are experimental data, dashed lines are the BEM [Lin, Newman, and Yue (1984); Wang, Chen and Tang (2009)] results and solid lines are the coupled mode results)
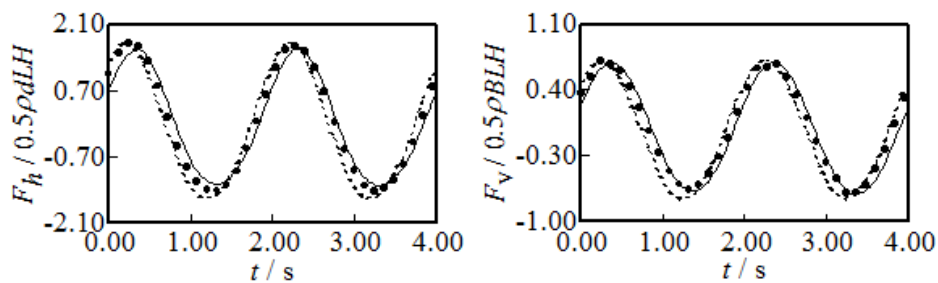
(a) Case1: T=2s, H=0.03m, d=0.27m
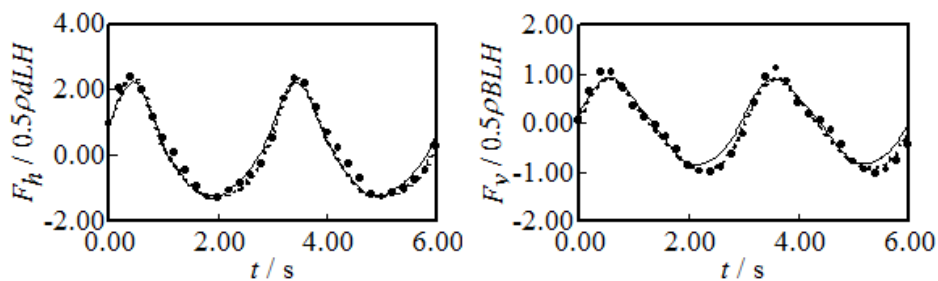
(b) Case2: T=3s, H=0.06m, d=0.24m

(c) T=5s, H=0.06m, d=0.24m

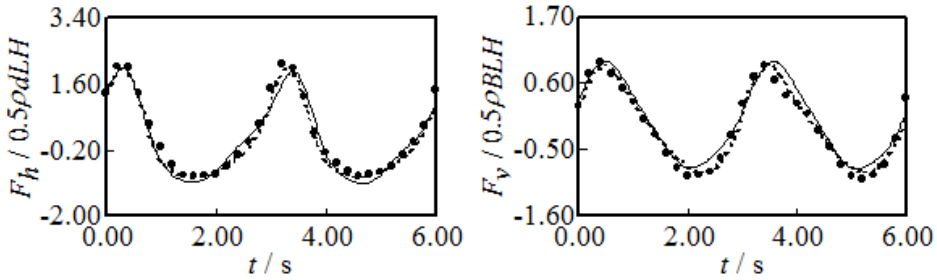(d) Case4: T=3s, H=0.06m, d=0.27m

(f) Case5: *T*=3s, *H*=0.06m, *d*=0.18m

Figure 11 : Time history of horizontal (left) and vertical (right) wave forces (where markers are the experimental data, dashed lines are the BEM [Lin, Newman, and Yue (1984); Wang, Chen and Tang (2009)] results and solid lines are the coupled mode results)

From Tab. 3, it can be seen that the computational time required by the present coupled model is over 60.33 times less than that of the boundary element method. Therefore, the present is more efficient.

9   Conclusions

A 2-D time-domain coupled model for nonlinear wave forces acting on a fixed ship section in a harbor has been developed in the present study. The whole domain is divided into the inner domain and the outer domain. The inner domain is the area around the ship, where flow is expressed by the Laplace equation and numerically solved by the boundary element method. The remaining area is the outer domain, where flow is described by the higher-order Boussinesq equations and numerically solved by the finite difference method. The matching conditions on the interfaces between the inner domain and the outer domain are the continuation of volume flux and the equality of wave elevations, which obeys mass conservation. The solution procedure and the calculation region of the inner domain are also discussed in detail in the paper.

The physical experiment, including the wave flume and the wave acting on a fixed ship, the boundary element method in complex [Lin, Newman, and Yue (1984); Wang, Chen and Tang (2009)] and the Boussinesq equations [Zou (1999)] are adopted to verify the present coupled model, and it can be seen that the numerical results of the present mode agree well with the experimental data and the other numerical results, but the computational efficiency of the present model is much

higher than that of boundary element method, so the coupled model is accurate and efficient, which can be used for the wave motions in a harbor with large area and is especially useful for the study of the effects of harbor boundaries and bottom on wave forces acting on a fixed ship in a harbor. Furthermore, based on the present model and the linear theory of the motions of floating structures, nonlinear wave forces acting on a ship moored in a harbor will be discussed in the future.

In addition, the present model can not only provide a reference for the coupled calculation, but also be applied to the district computation of wave field.

Acknowledgement

References

Bingham, H. B. (2000): A Hybrid Boussinesq-panel method for predicting the motion of a moored ship. *Coastal Engineering*, vol. 40, no. 1, pp. 21-38.

Boo, S.Y.; Kim, C. H.; Kim, M. H. (1994): A numerical wave tank for nonlinear irregular waves by 3-D higher order boundary element method. *International Journal of Offshore and Polar Engineering*, vol. 4, no. 4, pp. 265-272.

Celebl, M.S.; Kim, M. H.; Beck, R. F. (1998): Fully nonlinear 3-D numerical wave tank simulation. Journal of Ship Research, vol. 42, no. 1, pp. 33-45.

Jiang, T. (1998): Investigation of waves generated by ships in shallow water. *Proceedings of the 22th Symposium on Naval Hydrodynamics*, Washington, D. C., USA.

Hamidou, M.; Molin, B.; Kadri, M.; Kimmoun, Q.; Tahakourt, A. (2009): A coupling method between extended Boussinesq equations and the integral equation method with application to a two-dimensional numerical wave-tank. *Ocean Engingeering*, vol. 36, no. 17-18, pp. 1377-1385.

Hirt, C. W.; Nichols, B. D. (1981): Volume of Fluid (VOF) method for the dynamics of free boundaries. *Journal of Computational Physics*, vol. 39, no. 1, pp. 201-225.

Hsu, T. W.; Hsiao, S. C.; Ou, S. H.; Wang, S. K.; Yang, B. D.; Chou, S. E. (2007): An application of Boussinesq equations to Bragg reflection of irregular waves. *Ocean Engineering*, vol. 34, no.5-6, pp. 870-883.

Lin, W. M.; Newman, J. N.; Yue, D. K. (1984): Nonlinear forced motion of floating bodies. *Proceedings of the 15th Symp on Naval Hydrodynaics*, Hamburg, Germany, pp. 33-47.

Madsen, P. A.; Bingham, H. B.; Liu, H. (2002): A new Boussinesq method for fully nonlinear waves from shallow to deep water. *Journal of Fluid Mechanics*, Vol. 462, pp. 1-30.

Moulinec, C., Issa, R., Marongiu, J., Violeau, D. (2008): Parallel 3-D SPH Simulations. *Computer Modeling in Engineering and Sciences*, vol. 25, no. 3, pp. 133-147.

Nwogu, O. (1993): Alternative form of Boussinesq equations for nearshore wave propagation. *Journal of Waterway, Port, Coastal and Ocean Engineering*, vol. 119, no. 6, pp. 618–638.

Park, J. C.; Kim, M. H. (1998): Fully nonlinear wave-current-body interaction by a 3D viscous numerical wave tank. *Proceedings of the 8th International Offshore and Polar Engineering Conference*, Montreal, Canada.

Peregrine, D. H. (1967): Long waves on a beach. *Journal of Fluid Mechanics*, vol. 27, no. 4, pp. 815-827.

Qi, P.; Wang, Y. X.; Zou, Z. L. (2000): 2-D composite model for numerical simulations of nonlinear waves. *China Ocean Engineering*, vol. 14, no. 1, pp. 113-120.

Qi, P.; Zou, Z. L.; Wang, Y. X. (2000): A 3-D composite model for numerical simulation of nonlinear waves. *Proceedings of the Tenth International Offshore and Polar Engineering Conference*, Seattle, USA.

Takagi, K.; Naito, S.; Hirota, K. (1994): Hydrodynamic forces acting on a floating body in a harbour of arbitrary geometry. *Proc. 3nd Int. Offshore and Polar Engineering Conference*, pp. 192-199.

Turnbull, M. S.; Borthwick, A. G. L.; Eatock, Taylor. R. (2003): Wave-structure interaction using coupled structured-unstructured finite element meshes. *Applied Ocean Research*, vol. 25, no. 2, pp. 63-77.

Van Oortmerssen, G. (1976): The motions of a moored ship in waves. *Netherlands Ship Model Basin Publication* No. 510.

Wang, D. G.; Chen, X. F.; Tang, H. X. (2009): Time Stepping Solutions of Nonlinear Wave Forces on Ship Section in Harbor. *Journal of Ship Mechanics*, vol. 13, no. 3, pp. 357-368. (In China)

Wang, D. G.; Zou, Z. L. (2007): Study of non-linear wave motions and wave forces on ship sections. *Ocean Engineering*, vol. 34, no. 8-9, pp. 1245-1256.

Wang, D. G.; Zou, Z. L.; Liu, X. (2010): Fully nonlinear 3-D numerical wave

tank simulation. *Journal of Ship Mechanics*, vol. 14, no. 6, no. 577-586. (In China)

Wang, D. G.; Zou, Z. L.; Tham, L. G. (2011): A 3-D time-domain coupled model for nonlinear waves acting on a box-shaped ship fixed in a harbor. *China Ocean Engineering*, vol. 25, no. 3, pp. 441-456.

Wang, D. G.; Zou, Z. L.; Tham, L. G.; Liu, X. (2010): A time-domain coupled model for nonlinear wave forces on a fixed box-shaped ship in a harbor. *China Ocean Engineering*, vol. 24, no. 1, pp. 41-56.

Wei, G.; Kirby, J. T.; Grilli, S. T.; Subramanya, R. (1995): A fully nonlinear Boussinesq model for surface waves. Part1. Highly nonlinear unsteady waves. *Journal of Fluid Mechanics*, vol. 294, pp. 71-92.

Wu, G. X.; Eatock, Taylor. R. (1994): Finite element analysis of two-dimensional non-linear transient water waves. *Applied Ocean Research*, vol. 16, no. 6, pp. 363-372.

Zou, Z. L. (1999): Higher order Boussinesq equations. *Ocean Engineering*, vol. 26, no. 8, pp. 767-792.

Zou, Z. L.; Bowers, E. C. (1993): A mathematical Model Simulation of a ship Moored Against a Quay in Shoreham Harbor with Comparisons Against Physical Model and Field Data. *Report SR 378*, Hydraulic Research Wallingford, UK.

Zou, Z. L.; Xu, B. H. (1998): Numerical model for solving Boussinesq-type equations: comparison and validation. *Acta Oceanologica Sinica*, vol. 17, no. 3, pp. 375-386.